defined

$$A=\left(\frac{d\Gamma^{+}}{dE_{+}}-\frac{d\Gamma^{-}}{dE_{-}}\right)\Big/\left(\frac{d\Gamma^{+}}{dE_{+}}+\frac{d\Gamma^{-}}{dE_{-}}\right). \quad (17)$$

We give numerical estimates of the magnitude of A using $\delta_2=-10°$ and assuming maximal CP violation, i.e., $\phi=\frac{1}{2}\pi$. ξ is taken to be a constant and its magnitude is chosen to be 1, 4, and 20. The magnitude of A is given in Fig. 2 as a function of the charged-pion kinetic energy in the region of the neutral-pion pole. As can be seen, the magnitude of A can be relatively large over a sizable portion of the charged pion spectrum. In particular, on the basis of the η^0-pole model ($\xi\simeq 3$), the magnitude of A averages out to be $\approx 10\%$ over the region shown. The sign of A, however, remains undetermined since the sign of ξ and ϕ are not known. For nonmaximal CP violation, one has to multiply the asymmetries in Fig. 2 by $\sin\phi$. For $\phi \ll 1$, the resulting asymmetry as expected, would be quite small.

PHYSICAL REVIEW D VOLUME 3, NUMBER 9 1 MAY 1971

Bethe-Salpeter Solution for Nucleon-Nucleon Scattering with Pion Exchange in the $^1S_0$ and $^3P_0$ States*

J. L. GAMMEL, M. T. MENZEL, AND W. R. WORTMAN†
Los Alamos Scientific Laboratory, University of California, Los Alamos, New Mexico 87544
(Received 20 November 1970)

The Bethe-Salpeter equation is solved for nucleon-nucleon scattering in the ladder approximation with pion exchange for the $^1S_0$ and $^3P_0$ states with no approximations beyond use of a finite mesh. It is found that solutions exist without the need for any cutoff so long as the coupling constant $g^2/4\pi$ is between about -4 and $+7$ for the $^1S_0$ state and for $g^2/4\pi$ less than about $+4$ for the $^3P_0$ state. These results are in qualitative agreement with the predictions of Mandelstam. It is found that the Padé approximant as applied to the coefficients of the iteration solution provides an efficient alternative to the method of matrix inversion for solving the equations for a given mesh.

I. INTRODUCTION

THE Bethe-Salpeter (BS) equation[1] for nucleon-nucleon (NN) scattering is of physical interest for several reasons. It is a relativistic generalization of the Schrödinger equation and sums a limited set of graphs from field theory depending on the kernel. In fact, our original motivation for considering this problem was directed toward finding a means of generating the amplitudes for the individual ladder graphs. We will consider the ladder series with pion exchange for the $J=0$ case in this calculation.

The realistic BS equation[2] is difficult to deal with since it is generally in the form of coupled singular integral equations. Several authors[3] have considered various aspects of the spin-$\frac{1}{2}$-on-spin-$\frac{1}{2}$ problem. For the NN case, Gourdin[4] took advantage of the four-dimensional symmetry and expanded the wave function in hyperspherical harmonics. The result was an infinite set of scalar coupled equations in one continuous variable which were coupled in the quantum number associated with the fourth dimension. A solution was then obtained by taking only the lowest value for the quantum number. However, the effect of this approximation above the elastic threshold is not clear. Ito *et al.*[5] and Murota *et al.*[6] have approached this problem somewhat differently. They have used the kernel-subtraction method of Levine *et al.*[7] to reduce the singularity of the kernel and taken the approximation of neglecting negative-energy intermediate states. This leads to a single integral equation in two continuous variables plus an auxiliary integral equation in one variable. These equations are solved by matrix inversion with reasonable accuracy. However, the approximation of neglecting negative-energy states is probably poor since the pseudoscalar γ_5 interaction tends to strongly couple positive- and negative-energy states. Therefore in this calculation we will employ the methods of Murota *et al.*, but we will include all intermediate states.

Fortunately we are not completely ignorant as to what to expect for solutions to the BS equation.

* Work performed under the auspices of the U. S. Atomic Energy Commission.
† Present address: Service de Physique Théorique, CEN-Saclay, B. P. No. 2, 91 Gif-sur-Yvette, France.
[1] E. E. Salpeter and H. A. Bethe, Phys. Rev. **84**, 1232 (1951).
[2] A recent review is N. Nakanishi, Progr. Theoret. Phys. (Kyoto) Suppl. **43**, 1 (1969).
[3] J. Connell, Phys. Rev. **179**, 1374 (1969); P. Narayanswamy and A. Pagnamenta, Nuovo Cimento **53A**, 635 (1968); A. R. Swift and B. W. Lee, Phys. Rev. **131**, 1857 (1963).
[4] M. Gourdin, Nuovo Cimento **7**, 338 (1958).
[5] H. Ito, M. Mizouchi, T. Murota, T. Nakano, M.-T. Noda, and F. Tanaka, Progr. Theoret. Phys. (Kyoto) **37**, 372 (1967).
[6] T. Murota, M.-T. Noda, and F. Tanaka, Progr. Theoret. Phys. (Kyoto) **41**, 1251 (1969).
[7] M. Levine, J. Tjon, and J. Wright, Phys. Rev. Letters **16**, 962 (1966).

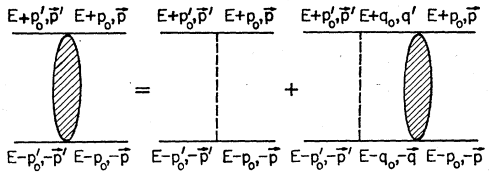

FIG. 1. Schematic representation of the BS equation.

Mandelstam[8] has analyzed the NN scattering problem for pseudoscalar exchange in the ladder approximation by examining the large-momentum behavior. He has reduced the BS equation to differential equations valid in the region of small r in coordinate space and looked at the behavior at the origin. On this basis he concludes that for a given state, unique solutions exist if and only if the coupling constant $g^2/4\pi$ (which is about 14 from NN scattering data) is less than some critical value. In particular, for the $^1S_0$ state, $g^2/4\pi<2\pi$, and for the $^3P_0$ state, $g^2/4\pi<\frac{1}{2}\pi$. In a solution with no approximations, one expects to find a behavior reflecting this limitation.

II. METHOD OF SOLUTION

A. Reduction of BS Equation

The BS equation in the ladder approximation is shown schematically in Fig. 1 where the energy and momentum of each line is indicated. For on-shell scattering, p_0 and p_0' will be taken as zero. The equation to be solved is

$$\phi=\frac{g^2}{4\pi}\frac{\gamma_5^{(1)}\gamma_5^{(2)}}{(p_0'-p_0)^2-(\mathbf{p}'-\mathbf{p})^2-\mu^2}-\frac{i}{4\pi^3}\int dq_0 d\mathbf{q}\left[\frac{g^2}{4\pi}\frac{\gamma_5^{(1)}\gamma_5^{(2)}}{(p_0'-q_0)^2-(\mathbf{p}'-\mathbf{q})^2-\mu^2}\right]\times\left[\frac{(E+q_0)\gamma_0^{(1)}-\mathbf{q}\cdot\boldsymbol{\gamma}^{(1)}+m}{(E+q_0)^2-E^2(q)}\times\frac{(E-q_0)\gamma_0^{(2)}+\mathbf{q}\cdot\boldsymbol{\gamma}^{(2)}+m}{(E-q_0)^2-E^2(q)}\right]\phi. \quad (1)$$

Here $E^2(p)=p^2+m^2$ and the superscripts refer to particle 1 or 2.

The Dirac matrices will be taken as the direct product of two sets of Pauli matrices such that $\gamma_0=\rho_z I_\sigma$, $\gamma_5=\rho_x I_\sigma$, and $\boldsymbol{\gamma}=i\rho_y\boldsymbol{\sigma}$.

There are four solutions to the free Dirac equation, two with positive energy and two with negative energy. We combine these solutions to form a 4×4 matrix with the positive-energy solutions in the first two columns and call the result Ψ. It can be shown that

$$\Psi=\left(I_\rho I_\sigma-i\rho_y\frac{\boldsymbol{\sigma}\cdot\mathbf{p}}{E(p)+m}\right)\left(\frac{E(p)+m}{2E(p)}\right)^{1/2} \quad (2)$$

and

$$\Psi\Psi^\dagger=I_\rho I_\sigma. \quad (3)$$

Therefore in terms of Ψ the Dirac equation becomes

$$p_0\gamma_0\Psi\gamma_0-\mathbf{p}\cdot\boldsymbol{\gamma}\Psi-m\Psi=0, \quad (4)$$

where $p_0=E(p)$ and the adjoint equation is

$$p_0\gamma_0\Psi^\dagger\gamma_0+\Psi^\dagger\mathbf{p}\cdot\boldsymbol{\gamma}-m\Psi^\dagger=0. \quad (5)$$

The curious appearance of the extra γ_0 is necessitated by the combining of positive- and negative-energy solutions.

Writing (1) as

$$\phi=G+GS\phi, \quad (6)$$

with G denoting the interaction and S the two-nucleon propagator, $\Psi(q)\Psi^\dagger(q)=I_\rho I_\sigma$ can be inserted between G and S. For particle 1,

$$\Psi^\dagger(q)\frac{(E+q_0)\gamma_0^{(1)}-\boldsymbol{\gamma}^{(1)}\cdot\mathbf{q}+m}{(E+q_0)^2-E^2(q)}=\frac{\Psi^\dagger(E+q_0)\gamma_0^{(1)}+E(q)\gamma_0^{(1)}\Psi^\dagger\gamma_0^{(1)}}{(E+q_0)^2-E^2(q)}=\frac{(E+q_0)+E(q)\gamma_0^{(1)}}{(E+q_0)^2-E^2(q)}\Psi^\dagger\gamma_0^{(1)}=\begin{bmatrix}\frac{1}{E+q_0-E(q)} & 0\\ 0 & \frac{1}{E+q_0+E(q)}\end{bmatrix}I_\sigma^{(1)}\Psi^\dagger\gamma_0^{(1)}\equiv S_\rho^{(1)}I_\sigma^{(1)}\Psi^\dagger\gamma_0^{(1)}. \quad (7)$$

Taking particle 2 into account in a similar manner, (6) can be written

$$\phi=G+G\Psi S_\rho^{(1)}S_\rho^{(2)}\Psi^\dagger\gamma_0\phi \quad (8)$$

or

$$\Psi^\dagger\gamma_0\phi\Psi=\Psi^\dagger\gamma_0G\Psi+\Psi^\dagger\gamma_0G\Psi S\Psi^\dagger\gamma_0\phi\Psi. \quad (9)$$

Here the arguments of the Ψ's are taken from Fig. 1, γ_0 and Ψ indicate the product of two such objects, one

TABLE I. ρ-spin states indicating positive or negative energy for particle 1 then particle 2.

States		Notation
Triplet	$++$	$+$
	$--$	$-$
	$\frac{1}{\sqrt{2}}(+-\oplus-+)$	e (even)
Singlet	$\frac{1}{\sqrt{2}}(+-\ominus-+)$	o (odd)

[8] S. Mandelstam, Proc. Roy. Soc. (London) **A237**, 496 (1956).

for each particle, and

$$S=S_\rho^{(1)}S_\rho^{(2)}=\left[\frac{1}{E+q_0-E(q)}\left(\frac{1+\rho_z^{(1)}}{2}\right)+\frac{1}{E+q_0+E(q)}\left(\frac{1-\rho_z^{(1)}}{2}\right)\right]\left[\frac{1}{E-q_0-E(q)}\left(\frac{1+\rho_z^{(2)}}{2}\right)+\frac{1}{E-q_0+E(q)}\left(\frac{1-\rho_z^{(2)}}{2}\right)\right]. \quad (10)$$

S is now independent of angle and spin σ. Introducing the notation $\phi=\Psi^\dagger\gamma_0\phi\Psi$ and $G=\Psi^\dagger\gamma_0 G\Psi$, the reduced equation is symbolically

$$\phi=G+GS\phi. \quad (11)$$

B. Interaction

The interaction G is

$$G=(g^2/4\pi)[\Psi^\dagger(q)^{(1)}\gamma_0^{(1)}\gamma_5^{(1)}\Psi(p)^{(1)}\times\Psi^\dagger(-q)^{(2)}\gamma_0^{(2)}\gamma_5^{(2)}\Psi(-p)^{(2)}]\times[(q_0-p_0)^2-(\mathbf{q}-\mathbf{p})^2-\mu^2]^{-1}. \quad (12)$$

Using (2) for Ψ, G is reduced to

$$G=(g^2/4\pi)\{(i\rho_y^{(1)})(i\rho_y^{(2)})[F^2+F\mathbf{B}\cdot(\boldsymbol{\sigma}^{(1)}+\boldsymbol{\sigma}^{(2)})+\mathbf{B}\cdot\boldsymbol{\sigma}^{(1)}\mathbf{B}\cdot\boldsymbol{\sigma}^{(2)}]-\tfrac{1}{2}(i\rho_y^{(1)}-i\rho_y^{(2)})[F(\boldsymbol{\sigma}^{(1)}+\boldsymbol{\sigma}^{(2)})\cdot\mathbf{A}+\mathbf{B}\cdot\boldsymbol{\sigma}^{(1)}\mathbf{A}\cdot\boldsymbol{\sigma}^{(2)}+\mathbf{B}\cdot\boldsymbol{\sigma}^{(2)}\mathbf{A}\cdot\boldsymbol{\sigma}^{(1)}]-\tfrac{1}{2}(i\rho_y^{(1)}+i\rho_y^{(2)})[-F(\boldsymbol{\sigma}^{(1)}-\boldsymbol{\sigma}^{(2)})\cdot\mathbf{A}+\mathbf{B}\cdot\boldsymbol{\sigma}^{(1)}\mathbf{A}\cdot\boldsymbol{\sigma}^{(2)}-\mathbf{B}\cdot\boldsymbol{\sigma}^{(2)}\mathbf{A}\cdot\boldsymbol{\sigma}^{(1)}]-I_\rho^{(1)}I_\rho^{(2)}[\boldsymbol{\sigma}^{(1)}\cdot\mathbf{A}\boldsymbol{\sigma}^{(2)}\cdot\mathbf{A}]\}N[(q_0-p_0)^2-(\mathbf{q}-\mathbf{p})^2-\mu^2]^{-1}. \quad (13)$$

The quantities occurring are

$$F=1+\frac{\mathbf{p}\cdot\mathbf{q}}{[E(p)+m][E(q)+m]},$$
$$\mathbf{B}=\frac{i\mathbf{q}\times\mathbf{p}}{[E(p)+m][E(q)+m]},$$
$$\mathbf{A}=\frac{\mathbf{p}}{E(p)+m}-\frac{\mathbf{q}}{E(q)+m}, \quad (14)$$

and

$$N=\frac{[E(p)+m][E(q)+m]}{4E(p)E(q)}.$$

Writing (13) in the compressed form

$$G=(g^2/4\pi)\{\rho_1X_1+\rho_2X_2+\rho_3X_3-\rho_4X_4\}\times N[(q_0-p_0)^2-(\mathbf{q}-\mathbf{p})^2-\mu^2]^{-1}, \quad (15)$$

it is seen that ρ_i acts only in the ρ space while X_i acts in the σ space, which is the usual spin space. The ρ spin is analogous to the σ spin except that instead of operating on spin-up and spin-down states, the ρ spin operates on positive- and negative-energy states in exactly the same manner. Singlet and triplet ρ-spin states can be formed by the usual combinations of two-particle states. In Table I the ρ-spin states are given. Table II indicates the results of ρ_i acting on these states.

TABLE II. Properties of the ρ_i operators.

State	Result of ρ_1	Result of ρ_2	Result of ρ_3	Result of ρ_4
$+$	$-$	$-\frac{1}{\sqrt{2}}(o)$	$\frac{1}{\sqrt{2}}(e)$	$+$
$-$	$+$	$-\frac{1}{\sqrt{2}}(o)$	$-\frac{1}{\sqrt{2}}(e)$	$-$
e	$-(e)$	zero	$-\frac{1}{\sqrt{2}}(+\ominus-)$	e
o	o	$\frac{1}{\sqrt{2}}(+\oplus-)$	zero	o

The properties of the X_i operators regarding spin and parity can be determined by observing the symmetry in $\sigma^{(1)}$ and $\sigma^{(2)}$ and by noting that $\boldsymbol{\sigma}$ and $\mathbf{B}$ are pseudovectors, $\mathbf{A}$ is a vector, and F is a scalar. The results are recorded in Table III. Odd parity indicates a parity-nonconserving transition and odd spin indicates singlet to triplet coupling.

C. Propagator

The propagator S is proportional to I_σ but it does not conserve ρ spin. Although S is diagonal in the representation $++,--,+-,-+$, this is no longer true for the representation of Table I. For this representation the S operator in ρ-spin space is given as

$$\begin{aligned}
(+|S|+)&=[E+q_0-E(q)+i\epsilon]^{-1},\\
&\quad\times[E-q_0-E(q)+i\epsilon]^{-1},\\
(-|S|-)&=[E+q_0+E(q)-i\epsilon]^{-1}\\
&\quad\times[E-q_0+E(q)-i\epsilon]^{-1},\\
(e|S|e)=(o|S|o)&=\tfrac{1}{2}\{[E+q_0-E(q)+i\epsilon]^{-1}\\
&\quad\times[E-q_0+E(q)-i\epsilon]^{-1}\\
&\quad+[E+q_0+E(q)-i\epsilon]^{-1}\\
&\quad\times[E-q_0-E(q)+i\epsilon]^{-1}\},\\
(o|S|e)=(e|S|o)&=\tfrac{1}{2}\{[E+q_0-E(q)+i\epsilon]^{-1}\\
&\quad\times[E-q_0+E(q)-i\epsilon]^{-1}\\
&\quad-[E+q_0+E(q)-i\epsilon]^{-1}\\
&\quad\times[E-q_0-E(q)+i\epsilon]^{-1}\}.
\end{aligned} \quad (16)$$

TABLE III. Properties of the X_i operators.

Operator	Parity	Spin
X_1	even	even
X_2	odd	even
X_3	odd	odd
X_4	even	even

D. Intermediate-State Analysis

Now (11) can be considered taken between appropriate states. In particular, we will consider the $^1S_0$ state. The desired quantity is $(^1S_0^+|\phi|^1S_0^+)$, where the + indicates a positive-energy state. The equation becomes

$$(\alpha|\phi|^1S_0^+)=(\alpha|G|^1S_0^+)$$
$$-\frac{i}{2\pi^2}\int dq_0 dq \sum_{\beta,\gamma}(\alpha|G|\beta)(\beta|S|\gamma)(\gamma|\phi|^1S_0^+). \quad (17)$$

Here α, β, and γ are appropriate states and β and γ are summed over for the intermediate states. In general, since the total angular momentum is conserved, there will be eight intermediate states, four each for $^1S_0$ and $^3P_0$ since there are four possible ρ spins for each. However, the character of the interaction will limit this number. The integration over angle in the homogeneous term has been carried out by using the addition theorem which is allowed since S is independent of angle and spin. In addition the definitions of G and ϕ have been shifted so that $(\alpha|G|\beta)=2p_\alpha p_\beta G$ and $(\alpha|\phi|\beta)=2p_\alpha p_\beta\phi$, which gives the different coefficient for the homogeneous term relative to (1).

Possible intermediate states β and γ are now to be determined by the nature of the interaction and the S operator. Of course, α must take on all the values that γ takes on in order to give a complete set of equations. Taking α as $^1S_0^+$, ρ_1X_1 gives $\beta=^1S_0^-$ and S gives $\gamma=^1S_0^-$; ρ_2X_2 gives nothing; ρ_3X_3 gives $\beta=^3P_0^e$ and S gives $\gamma=^3P_0^e$ or $^3P_0^o$. Finally, ρ_4X_4 gives $\beta=^1S_0^+$ and S leads to $\gamma=^1S_0^+$. Now we must consider $\alpha=^1S_0^-$, $^3P_0^e$, and $^3P_0^o$ to see if additional γ's are found. The result is that no other states appear.

This indicates that four coupled equations in two continuous variables are required. Introducing the notation $\phi(p,p_0,\alpha)=(\alpha|\phi|^1S_0^+)$, $G(p,p_0,\alpha,q,q_0,\beta)=(\alpha|G|\beta)$, and $S(q,q_0,\beta,\gamma)=(\beta|S|\gamma)$ and labeling the states $^1S_0^+$, $^1S_0^-$, $^3P_0^e$, $^3P_0^o$ as 1, 2, 3, 4, respectively, the equations are

$$\phi(p,p_0,\alpha)=G(p,p_0,\alpha,\hat{p},0,1)$$
$$-\frac{i}{2\pi^2}\int dq dq_0 \sum_{\beta,\gamma} G(p,p_0,\alpha,q,q_0,\beta)$$
$$\times S(q,q_0,\beta,\gamma)\phi(q,q_0,\gamma), \quad (18)$$

where $\hat{p}=(E^2-m^2)^{1/2}$ is the momentum in the center-of-mass system. Now $\phi(\hat{p},0,1)$ is essentially the T matrix describing the desired on-shell $^1S_0^+\rightarrow{}^1S_0^+$ transition.

The input for the calculation is the quantity $G(p,p_0,\alpha,q,q_0,\beta)$. These elements are found by taking matrix elements of the operator G from (15) between states of either $|^1S_0)=\chi_s$ or $|^3P_0)=\mathbf{p}\cdot\boldsymbol{\chi}/p$, where $\boldsymbol{\chi}$ is written as a Cartesian vector with components

$$\chi_x=(\beta\beta-\alpha\alpha)/\sqrt{2},$$
$$\chi_y=i(\beta\beta+\alpha\alpha)/\sqrt{2},$$
$$\chi_z=(\alpha\beta+\beta\alpha)/\sqrt{2}, \quad (19)$$

and

$$\chi_s=(\alpha\beta-\beta\alpha)/\sqrt{2}.$$

α and β denote the usual spin up and spin down. For example, consider $G(p,p_0,1,q,q_0,1)$. For this, $(^1S_0^+|G|^1S_0^+)$ is required and since it is a $+\rightarrow+$ transition, only ρ_4 will contribute. Therefore

$$G(p,p_0,1,q,q_0,1)$$
$$=\frac{g^2}{4\pi}\times\frac{1}{2}\int_{-1}^{1}d(\cos\theta)\{-(+|\rho_4|+)\chi_s^\dagger\boldsymbol{\sigma}^{(1)}\cdot\mathbf{A}\boldsymbol{\sigma}^{(2)}\cdot\mathbf{A}\chi_s$$
$$\times 2pqN[(q_0-p_0)^2-(\mathbf{q}-\mathbf{p})^2-\mu^2]^{-1}\}. \quad (20)$$

Carrying out the calculation of the spin part of the matrix element,

$$\chi_s^\dagger\boldsymbol{\sigma}^{(1)}\cdot\mathbf{A}\boldsymbol{\sigma}^{(2)}\cdot\mathbf{A}\chi_s$$
$$=\chi_s^\dagger\boldsymbol{\sigma}^{(1)}\cdot\mathbf{A}[-\mathbf{A}\cdot\boldsymbol{\chi}]$$
$$=\chi_s^\dagger[-\mathbf{A}\cdot\mathbf{A}\chi_s-i\mathbf{A}\times\mathbf{A}\cdot\boldsymbol{\chi}]=-\mathbf{A}^2. \quad (21)$$

TABLE IV. Elements of $(\alpha(p)|G|\beta(q))\times 2E(p)E(q)\times 4\pi/g^2$.

α \ β	$^1S_0^+$	$^1S_0^-$	$^3P_0^e$	$^3P_0^o$
$^1S_0^+$	$-[E(p)E(q)-m^2]Q_0+pqQ_1$	$-[E(p)E(q)+m^2]Q_0-pqQ_1$	$-\sqrt{2}(mqQ_0-mpQ_1)$	0
$^1S_0^-$	$-[E(p)E(q)+m^2]Q_0-pqQ_1$	$-[E(p)E(q)-m^2]Q_0+pqQ_1$	$\sqrt{2}(mqQ_0-mpQ_1)$	0
$^3P_0^e$	$-\sqrt{2}(mpQ_0-mqQ_1)$	$\sqrt{2}(mpQ_0-mqQ_1)$	$2(pqQ_0+m^2Q_1)$	0
$^3P_0^o$	0	0	0	$-2E(p)E(q)Q_1$

Therefore since $(+|\rho_4|+)=1$,

$$G(p,p_0,1,q,q_0,1)$$
$$=\frac{g^2}{4\pi}\times\frac{1}{2}\int_{-1}^{1}d(\cos\theta)\frac{2pq\mathbf{A}^2N}{(q_0-p_0)^2-q^2-p^2-\mu^2+2pq\cos\theta}$$
$$=\frac{g^2}{4\pi}\times\frac{1}{2}\int_{-1}^{1}d(\cos\theta)\times\frac{\{2[E(p)E(q)-m^2-pq\cos\theta]/[E(p)+m][E(q)+m]\}\{[E(p)+m][E(q)+m]/4E(p)E(q)\}}{-\{[p^2+q^2+\mu^2-(p_0-q_0)^2]/2pq-\cos\theta\}}$$
$$=\frac{g^2}{4\pi}\frac{1}{2E(p)E(q)}\{-[E(p)E(q)-m^2]Q_0(z)+pqQ_1(z)\}. \tag{22}$$

Here $Q_l(z)$ is the Legendre function of the second kind of order l and the argument is

$$z=[p^2+q^2+\mu^2-(p_0-q_0)^2]/2pq. \tag{23}$$

Carrying out the calculation of the other matrix elements, the results in Table IV are found.

E. Kernel Subtraction

The resulting set of equations is singular due to the presence of $S(q,q_0,1,1)$. From (16) it is apparent that $(+|S|+)$ has poles which lie on either side of the q_0 integration contour and which coincide when the two particles are on the mass shell leading to the expected branch cut from unitarity. This difficulty cannot be avoided but it can be subdued by the kernel subtraction method of Levine *et al.* This method replaces the original equation with another in which the effective interaction vanishes at the double pole. ϕ' is defined as

$$\phi(p,p_0,\alpha)=t\phi'(p,p_0,\alpha), \tag{24}$$

where t is independent of p, p_0, and α and is fixed by requiring

$$\phi'(\hat{p},0,1)=G(\hat{p},0,1\,\hat{p},0,1). \tag{25}$$

Substituting this into (18),

$$t\phi'(p,p_0,\alpha)=G(p,p_0,\alpha,\hat{p},0,1)-\frac{i}{2\pi^2}t\int dq_0dq\sum_{\beta,\gamma}G(p,p_0,\alpha,q,q_0,\beta)S(q,q_0,\beta,\gamma)\phi'(q,q_0,\gamma). \tag{26}$$

Using (25),

$$t=\frac{G(\hat{p},0,1,\hat{p},0,1)}{G(\hat{p},0,1,\hat{p},0,1)+(i/2\pi^2)\int dqdq_0\sum_{\beta,\gamma}G(\hat{p},0,1,q,q_0,\beta)S(q,q_0,\beta,\gamma)\phi'(q,q_0,\gamma)}. \tag{27}$$

Introducing this result into (26), the equation for ϕ' is

$$\phi'(p,p_0,\alpha)=G(p,p_0,\alpha,\hat{p},0,1)-\frac{i}{2\pi^2}\int dqdq_0\sum_{\beta,\gamma}\left[G(p,p_0,\alpha,q,q_0,\beta)-\frac{G(p,p_0,\alpha,\hat{p},0,1)G(\hat{p},0,1,q,q_0,\beta)}{G(\hat{p},0,1,\hat{p},0,1)}\right]\times S(q,q_0,\beta,\gamma)\phi'(q,q_0,\gamma). \tag{28}$$

Now when $q=\hat{p}$ and $q_0=0$, that is, for internal nucleons on shell, the effective interaction vanishes for $\beta=1$ which is the ${}^1S_0{}^+$ state. While the equation for ϕ' is still singular, it is not as singular as that for ϕ and it can be handled using standard methods.

From (16) it is seen that $(+|S|+)$, $(-|S|-)$, $(e|S|e)$, and $(o|S|o)$ are even in q_0, while $(o|S|e)$ is odd. Since $G(p,p_0,\alpha,q,q_0,\beta)$ is dependent on p_0 and q_0 only through (23), which contains $(p_0-q_0)^2$, it is apparent that $\phi'(q,q_0,\alpha)$ is even in q_0 for $\alpha=1,2,3$ and odd in q_0 for $\alpha=4$. Consequently the q_0 integration can be changed to the interval $(0,\infty)$. That is, if K is defined as

$$K(p,p_0,\alpha,q,q_0,\beta)=\tfrac{1}{2}[G(p,p_0,\alpha,q,q_0,\beta)+G(p,p_0,\alpha,q,-q_0,\beta)]-\frac{G(p,p_0,\alpha,\hat{p},0,1)G(\hat{p},0,1,q,q_0,\beta)}{G(\hat{p},0,1,\hat{p},0,1)} \tag{29}$$

for $\alpha,\beta=1,2,3$ and

$$K(p,p_0,4,q,q_0,4) = \tfrac{1}{2}[G(p,p_0,4,q,q_0,4)-G(p,p_0,4,q,-q_0,4)],$$

then (28) can be written

$$\phi'(p,p_0,\alpha)=G(p,p_0,\alpha,\hat{p},0,1) - \frac{i}{\pi^2}\int_0^\infty dq\int_0^\infty dq_0 \sum_{\beta,\gamma} K(p,p_0,\alpha,q,q_0,\beta) \times S(q,q_0,\beta,\gamma)\phi'(q,q_0,\gamma). \quad (30)$$

F. Wick Rotation

The Wick rotation[9,10] can now be carried out changing the q_0 integration to an iq_4 integration by a 90° rotation of the q_0 contour. Of course, singularities so encountered must be accounted for. The propagators S can have poles in the path of the rotation. Consider for example

$$S(q,q_0,1,1) = [E+q_0-E(q)+i\epsilon]^{-1}[E-q_0-E(q)+i\epsilon]^{-1}. \quad (31)$$

The poles in the q_0 plane are shown in Fig. 2. The first factor gives a pole at $q_0=E(q)-E-i\epsilon$ and the second factor at $q_0=E-E(q)+i\epsilon$. Therefore the pole in the upper half-plane will be encountered if $E(q)<E$ (or equivalently if $q<\hat{p}$) by the indicated contour rotation at $q_0=E-E(q)$. Consequently, when (30) is Wick-rotated, it leads to a similar equation with an additional contribution from the poles. The result is

$$\phi'(p,ip_4,\alpha)=G(p,ip_4,\alpha,\hat{p},0,1) + \frac{1}{\pi^2}\int_0^\infty dq\int_0^\infty dq_4 \sum_{\beta,\gamma} K(p,ip_4,\alpha,q,iq_4,\beta) \times S(q,iq_4,\beta,\gamma)\phi'(q,iq_4,\gamma) + \frac{1}{\pi}\int_0^{\hat{p}} dq \sum_{\beta,\gamma} K(p,ip_4,\alpha,q,E-E(q),\beta) \times S_R(q,E-E(q),\beta,\gamma)\phi'(q,E-E(q),\gamma), \quad (32)$$

where $S_R(q,E-E(q),\beta,\gamma)$ is twice the residue at the pole. In particular,

$$S_R(q,E-E(q),1,1)=1/[E(q)-E],$$
$$S_R(q\,E-E(q),2,2)=0.0,$$
$$S_R(q,E-E(q),3,3)=S_R(q,E-E(q),4,4) = -1/2E, \quad (33)$$

and

$$S_R(q,E-E(q),3,4)=S_R(q,E-E(q),4,3) = -1/2E.$$

[9] G. C. Wick, Phys. Rev. **96**, 1124 (1954).
[10] N. Kemmer and A. Salam, Proc. Roy. Soc. (London) **A230**, 266 (1955).

The appearance of $\phi'(q,E-E(q),\gamma)$ in (32) requires the introduction of the auxiliary equation

$$\phi'(p,E-E(p),\alpha)=G(p,E-E(p),\alpha,\hat{p},0,1) + \frac{1}{\pi^2}\int_0^\infty dq\int_0^\infty dq_4 \sum_{\beta,\gamma} K(p,E-E(p),\alpha,q,iq_4,\beta) \times S(q,iq_4,\beta,\gamma)\phi'(q,iq_4,\gamma) + \frac{1}{\pi}\int_0^{\hat{p}} dq \sum_{\beta,\gamma} K(p,E-E(p),\alpha,q,E-E(q),\beta) \times S_R(q,E-E(q),\beta,\gamma)\phi'(q,E-E(q),\gamma). \quad (34)$$

Now (32) and (34) constitute a complete set of equations to be solved for $\phi'(p,ip_4,\alpha)$. These consist of eight coupled equations, four in two variables and four in one variable.

All quantities which appear in these equations are purely real or purely imaginary. This can be deduced by noting the symmetry with respect to p_0 and q_0. For example, $K(p,ip_4,\alpha,q,iq_4,\beta)$ and $S(q,iq_4,\alpha,\alpha)$ are strictly real while $S(q,iq_4,3,4)$ is purely imaginary. As a consequence, $\phi'(q,iq_4,\alpha)$ is real except for $\alpha=4$, where it is imaginary. Therefore by appropriate factoring out of i where it occurs, the equations become strictly real.

G. Phase Shift

In order to find the phase shift, the scattering amplitude ϕ is required. The program thus far has been devoted to solving for ϕ' so that given ϕ', (24) must be used to find ϕ. The result is

$$\phi(\hat{p},0,1)=\frac{G^2(\hat{p},0,1,\hat{p},0,1)}{G(\hat{p},0,1,\hat{p},0,1)-I}, \quad (35)$$

where after Wick rotation,

$$I=\frac{1}{\pi^2}\int_0^\infty dq\int_0^\infty dq_4 \sum_{\beta,\gamma} G(\hat{p},0,1,q,iq_4,\beta) \times S(q,iq_4,\beta,\gamma)\phi'(q,iq_4,\gamma) + \frac{1}{\pi}\int_0^{\hat{p}} dq \sum_{\beta,\gamma} G(\hat{p},0,1,q,E-E(q),\beta) \times S_R(q,E-E(q),\beta,\gamma)\phi'(q,E-E(q),\gamma). \quad (36)$$

I contains the unitary cut and thus to extract the tangent of the phase shift, a principal value must be taken. The result is

$$\tan\delta=\frac{E}{2\hat{p}}\frac{G^2(\hat{p},0,1,\hat{p},0,1)}{G(\hat{p},0,1,\hat{p},0,1)-\mathcal{P}I}, \quad (37)$$

where $\mathcal{P}$ denotes the principal value. Following

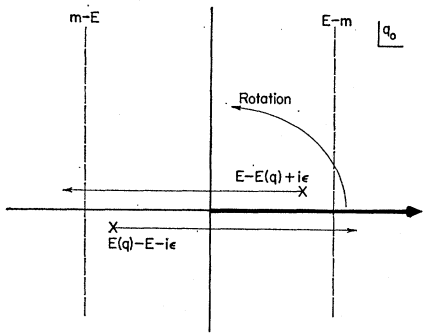

FIG. 2. Poles of the propagator $S(q,q_0,1,1)$ and the path of the Wick rotation.

Murota *et al.*,

$$\mathcal{P}I=\int_0^\infty dq\frac{\mathcal{P}}{E(q)^2-E^2}F(q)\,, \tag{38}$$

where

$$F(q)=\frac{1}{\pi^2}\int_0^\infty dq_4\sum_{\beta,\gamma}G(\hat{p},0,1,q,iq_4,\beta)S(q,iq_4,\beta,\gamma)$$
$$\times[E(q)^2-E^2]\phi'(q,iq_4,\gamma)$$
$$+\theta(\hat{p}-q)\frac{1}{\pi}\sum_{\beta,\gamma}G(\hat{p},0,1,q,E-E(q),\beta)$$
$$\times S_R(q,E-E(q),\beta,\gamma)[E(q)^2-E^2]$$
$$\times\phi'(q,E-E(q),\gamma)\,. \tag{39}$$

Now

$$F(\hat{p})=(E/\pi)G(\hat{p},0,1,\hat{p},0,1)\phi'(\hat{p},0,1)\,, \tag{40}$$

and the principal value is

$$\mathcal{P}I=\int_0^\infty dq\frac{1}{E(q)^2-E^2}[F(q)-F(\hat{p})]\,. \tag{41}$$

The program for solving for tan $\delta(^1S_0)$ is now complete. The same procedure can be carried out for the $^3P_0$ case and the result is very similar. In fact, if the labels $^1S_0$ and $^3P_0$ in Table IV are interchanged and if Q_0 and Q_1 are also interchanged, exactly the $^3P_0$ result is found. Therefore once the $^1S_0$ case is set up, the computation of the $^3P_0$ case is achieved simply by interchanging Q_0 and Q_1.

H. Numerical Procedure

Equations (32) and (34) are solved by first making a change of variable to change the integration intervals to $(-1,+1)$ and then using Simpson's rule to reduce the equations to a set of linear equations which are solved by matrix inversion. The q variable is changed to u by

$$q=[(1+u)/(1-u)](\hat{p}+50) \tag{42}$$

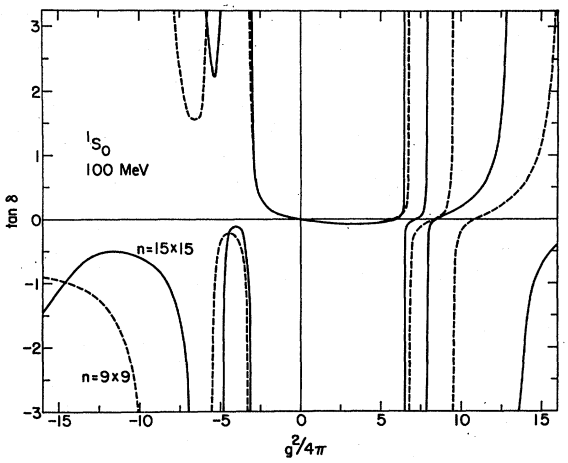

FIG. 3. $^1S_0$ tanδ as a function of $g^2/4\pi$ for different mesh sizes n at 100 MeV.

for the twofold integrals, and

$$q=(1+u)\hat{p}/2 \tag{43}$$

for the integration from 0 to $\hat{p}$. The q_4 integrals are transformed by

$$q_4=[(1+v)/(1-v)^\beta]q_{4m}\,, \tag{44}$$

where

$$\beta=1+\frac{\ln(\mu/q_{4m})}{\ln(1/\Delta)}\,. \tag{45}$$

Here Δ is the step size for Simpson's rule and μ is the pion mass. The parameter q_{4m} is chosen according to

$$q_{4m}=\begin{cases}|E(q)-E|+10 & \text{if } |E(q)-E|+10<\mu\\ \mu & \text{otherwise.}\end{cases} \tag{46}$$

This prescription gives a value of q_4 at $v=1-\Delta$ which is independent of q. Units are all taken as MeV and the parameters 50 in (42) and 10 in (46) are somewhat arbitrary.

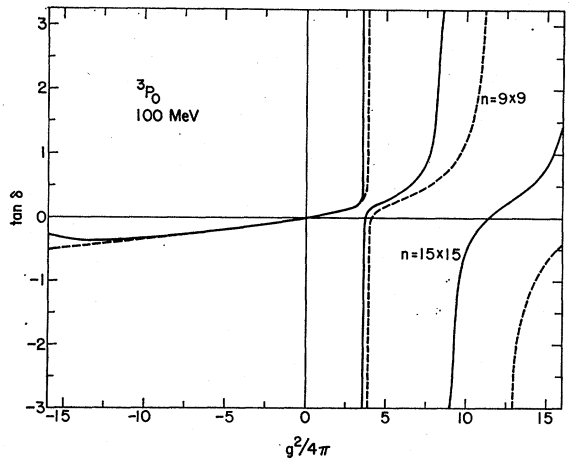

FIG. 4. $^3P_0$ tanδ as a function of $g^2/4\pi$ for different mesh sizes n at 100 MeV.

TABLE V. Padé method compared to matrix inversion at 100 MeV for the $^1S_0$ state.

Mesh	9×9	15×15	9×9	15×15
$g^2/4\pi$	1		4	
[1,1]	-3.399×10^{-2}	-3.372×10^{-2}	-8.351×10^{-2}	-8.293×10^{-2}
[5,5]	$-3.353\,430\,5\times10^{-2}$	$-3.310\,037\,8\times10^{-2}$	-6.019×10^{-2}	-5.515×10^{-2}
[10,10]	$-3.353\,430\,5\times10^{-2}$	$-3.310\,037\,8\times10^{-2}$	$-5.943\,681\,1\times10^{-2}$	$-5.494\,922\,9\times10^{-2}$
[15,15]	$-3.353\,430\,5\times10^{-2}$	$-3.310\,037\,8\times10^{-2}$	$-5.943\,681\,1\times10^{-2}$	$-5.494\,922\,9\times10^{-2}$
[19,19]	$-3.353\,430\,5\times10^{-2}$	$-3.310\,037\,8\times10^{-2}$	$-5.943\,681\,1\times10^{-2}$	$-5.494\,922\,9\times10^{-2}$
Matrix inversion	$-3.353\,430\,5\times10^{-2}$	...	$-5.943\,681\,0\times10^{-2}$	...
$g^2/4\pi$	7		10	
[1,1]	-1.074×10^{-1}	-1.048×10^{-1}	-1.204×10^{-1}	-1.171×10^{-1}
[5,5]	-1.276×10^{-1}	3.252×10^{-2}	1.266×10^{-1}	4.421×10^{-1}
[10,10]	$-2.724\,4\times10^{-1}$	-5.127×10^{-3}	-2.090×10^{-1}	1.974×10^{-1}
[15,15]	$-2.726\,178\,8\times10^{-1}$	-3.5605×10^{-3}	$-1.662\,56\times10^{-1}$	$2.067\,06\times10^{-1}$
[19,19]	$-2.726\,178\,7\times10^{-1}$	$-3.560\,75\times10^{-3}$	$-1.662\,23\times10^{-1}$	$2.066\,94\times10^{-1}$
Matrix inversion	$-2.726\,178\,9\times10^{-1}$	...	$-1.662\,619\,8\times10^{-1}$	...

The integrands vanish for $q=0$ and $q=\infty$ and also for $q_4=\infty$. Consequently an n-point mesh is effectively an $(n-2)$-point mesh for q and effectively an $(n-1)$-point mesh for q_4.

The matrix-inversion approach to solving the equations is adequate but it is rather slow. This is chiefly because they must be solved for a single value of $g^2/4\pi$. A possible alternative has been tried to overcome this problem. In particular, the equations are iterated using the desired mesh and the resulting coefficients of $(g^2/4\pi)^n$ in the series for $\tan\delta$ are found by expanding (37) appropriately. This series in then used to form the Padé approximant.[11] The $[N,N]$ Padé approximant is of the form

$$[N,N]=\sum_{n=1}^{N}\left(\frac{g^2}{4\pi}\right)^n A_n \Big/ \sum_{m=0}^{N}\left(\frac{g^2}{4\pi}\right)^m B_m, \qquad (47)$$

and the quantities A_n and B_m are determined by requiring that the series expansion of $[N,N]$ has exactly the same first $2N+1$ coefficients as the perturbation expansion. It is found that by using a suitably large value of N, which depends on $g^2/4\pi$, the value of the $[N,N]$ Padé approximant converges to the value of $\tan\delta$ found by matrix inversion for the same mesh. On this rather empirical basis, it is concluded that this use of the Padé method is an efficient alternative to the matrix-inversion method of solving this set of linear equations for a given mesh. No other significance is attached to this result because the higher-order terms from the perturbation expansion are severely mesh-dependent. Consequently nothing can be said concerning the ability of the Padé method to sum the actual perturbation series.

TABLE VI. Padé method compared to matrix inversion at 100 MeV for the $^3P_0$ state.

Mesh	9×9	15×15	9×9	15×15
$g^2/4\pi$	1		2	
[1,1]	4.518×10^{-2}	4.519×10^{-2}	9.613×10^{-2}	9.617×10^{-2}
[5,5]	$4.547\,716\,3\times10^{-2}$	$4.544\,057\,4\times10^{-2}$	$9.977\,077\,9\times10^{-2}$	$9.922\,209\,4\times10^{-2}$
[10,10]	$4.547\,716\,3\times10^{-2}$	$4.544\,057\,4\times10^{-2}$	$9.977\,078\,0\times10^{-2}$	$9.922\,209\,2\times10^{-2}$
[15,15]	$4.547\,716\,3\times10^{-2}$	$4.544\,057\,4\times10^{-2}$	$9.977\,078\,0\times10^{-2}$	$9.922\,209\,2\times10^{-2}$
[19,19]	$4.547\,716\,3\times10^{-2}$	$4.544\,057\,4\times10^{-2}$	$9.977\,078\,0\times10^{-2}$	$9.922\,209\,2\times10^{-2}$
Matrix inversion	$4.547\,716\,3\times10^{-2}$	...	$9.977\,078\,0\times10^{-2}$	...
$g^2/4\pi$	4		6	
[1,1]	2.203×10^{-1}	2.206×10^{-1}	3.871×10^{-1}	3.879×10^{-1}
[5,5]	-2.2962×10^{-1}	1.584×10^{-1}	3.1106×10^{-1}	4.2017×10^{-1}
[10,10]	$-2.293\,194\,7\times10^{-1}$	$1.583\,325\,0\times10^{-1}$	$3.112\,177\,3\times10^{-1}$	$4.198\,34\times10^{-1}$
[15,15]	$-2.293\,194\,7\times10^{-1}$	$1.583\,325\,0\times10^{-1}$	$3.112\,177\,3\times10^{-1}$	$4.198\,316\,1\times10^{-1}$
[19,19]	$-2.293\,194\,7\times10^{-1}$	$1.583\,325\,0\times10^{-1}$	$3.112\,177\,3\times10^{-1}$	$4.198\,316\,1\times10^{-1}$
Matrix inversion	$-2.293\,194\,8\times10^{-1}$	...	$3.112\,177\,3\times10^{-1}$	...

[11] *The Padé Approximant in Theoretical Physics*, edited by G. A. Baker, Jr. and J. L. Gammel (Academic, New York, 1970).

TABLE VII. Values of $g^2/4\pi$ for the first pole in tanδ for a mesh of 9×9.

Energy (MeV)	Positions of first poles, $^1S_0$		Position of first pole, $^3P_0$
5	−4.2	+8.2	+6.7
10	−4.0	+7.7	+5.8
25	−3.4	+6.9	+4.7
50	−3.2	+6.7	+4.1
100	−3.2	+6.8	+3.9
150	−3.2	+7.2	+3.8
200	−3.3	···	+3.8
250	−3.3	···	+3.8

III. RESULTS

The assertion that the Padé method leads to the same solution as the matrix-inversion method is demonstrated by Tables V and VI. For the larger coupling constants, the convergence of the Padé method is slower but the desired accuracy is always achieved. The computation was done using a nucleon mass of 938 MeV and a pion mass of 138 MeV.

Tables V and VI show that the solution for larger coupling constants is not independent of the mesh. This is demonstrated more clearly in Fig. 3 and 4.

From Fig. 3 and 4 it is seen that beyond a particular value of $g^2/4\pi$ where the first pole appears, the solutions become mesh dependent and the density of poles in this region increases with mesh size. The position of the first pole is somewhat energy dependent and it is given in Table VII.

There is a range of coupling constants for which the solution appears to be substantially independent of the mesh and these solutions are shown in Figs. 5 and 6.

The iteration procedure gives the coefficients of $(g^2/4\pi)^n$ in the series expansion of tanδ and so provides the amplitudes of the various-order ladder graphs. However the use of a finite mesh give increasingly limited accuracy for increasing orders. The coefficients found by this method are given in Table VIII. The first three coefficients have been calculated by independent direct evaluation of the amplitudes from the corresponding Feynman graphs and found to agree with the iteration results. The coefficients have also been found by using a finite-difference method on the solution by matrix inversion.

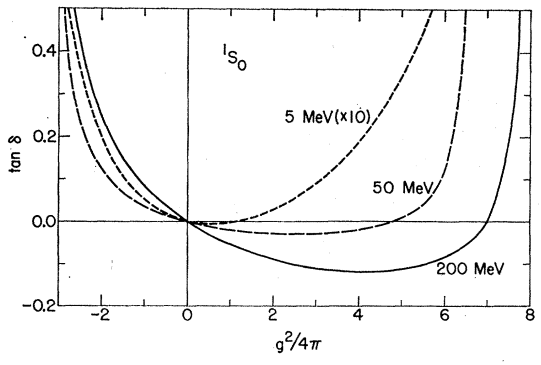

FIG. 5. $^1S_0$ tanδ as a function of $g^2/4\pi$ for different laboratory energies E.

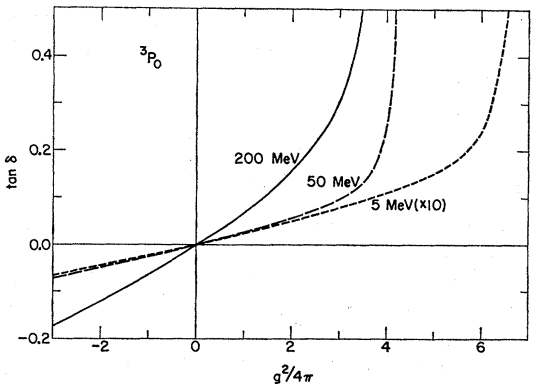

FIG. 6. $^3P_0$ tanδ as a function of $g^2/4\pi$ for different laboratory energies E.

For comparison with Murota *et al.*, the dependence of $\phi'(q,iq_4,1)$ on q and q_4 is shown in Fig. 7. Although ϕ' is still large at the last plotted values of q and q_4, this has no effect on the solution of the equations because

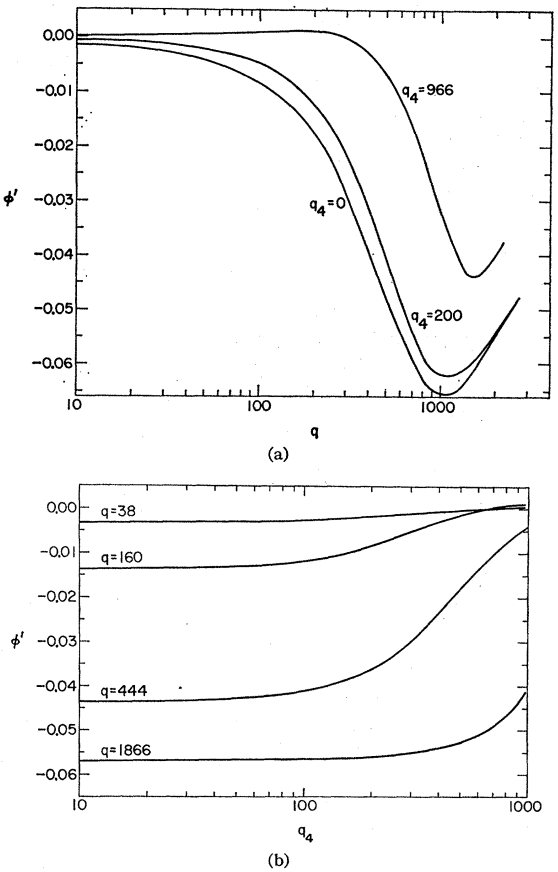

FIG. 7. $\phi'(q,iq_4,1)$ as a function of q and q_4 for the $^1S_0$ state at 100 MeV for a mesh of 9×9 at $g^2/4\pi=1$.

TABLE VIII. Coefficients A_n of $\tan\delta=\sum A_n(g^2/4\pi)^n$ at 100 MeV.

Order n	$^1S_0$ coefficients 9×9 mesh	$^1S_0$ coefficients 15×15 mesh	$^3P_0$ coefficients 9×9 mesh	$^3P_0$ coefficients 15×15 mesh
1	-4.2628×10^{-2}	-4.2628×10^{-2}	4.2628×10^{-2}	4.2628×10^{-2}
2	$+1.0828\times10^{-2}$	1.1256×10^{-2}	2.4103×10^{-3}	2.4199×10^{-3}
3	-2.2641×10^{-3}	-2.2272×10^{-3}	3.5151×10^{-4}	3.1944×10^{-4}
4	$+6.8932\times10^{-4}$	6.4615×10^{-4}	6.6687×10^{-5}	5.6520×10^{-5}
5	-2.0946×10^{-4}	-1.9332×10^{-4}	1.5416×10^{-5}	1.2319×10^{-5}
6	$+6.5968\times10^{-5}$	6.1115×10^{-5}	3.8214×10^{-6}	3.0878×10^{-6}

the interaction and the nucleon propagators fall off very fast at infinity.

Although all results presented in this section have been found using the complete set of equations, it is also found that very similar results are obtained if the contribution of the $^3P_0{}^o$ intermediate state is neglected. This is in agreement with the result of Noda[12] and is shown by Fig. 8.

IV. CONCLUSIONS

We have shown that it is possible to solve the Bethe-Salpeter equation for nucleon-nucleon scattering in the ladder approximation with pion exchange without introducing any cutoff so long as the coupling constant $g^2/4\pi$ does not exceed some critical value. The cutoff dependence is tested by use of different meshes in solving the equations.

Numerically it is found that for our meshes the $^1S_0$ equations have a solution only if the coupling constant $g^2/4\pi$ is confined between about -4 and about $+7$. The $^3P_0$ equations have a solution only if $g^2/4\pi$ is less than about $+4$. These critical values are mild functions of the energy as indicated in Table VII. Mandelstam's arguments indicate that the equations will have a unique solution if and only if the coupling constant is $-\frac{1}{2}\pi<g^2/4\pi<2\pi$ for the $^1S_0$ state and if $-2\pi<g^2/4\pi<\frac{1}{2}\pi$ for the $^3P_0$ state. These results are independent of energy. Our results are in qualitative agreement with Mandelstam's predictions and do not contradict them in that solutions are always found within these limits. In order to test these predictions accurately, it would be necessary to use much finer meshes. Unfortunately the enormous computer storage requirement limits the practical mesh size.

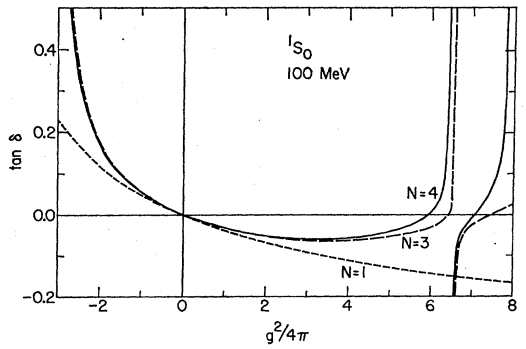

FIG. 8. $^1S_0$ $\tan\delta$ at 100 MeV for a 15×15 mesh for the full solution, $N=4$; for the solution neglecting the $^3P_0{}^o$ intermediate state, $N=3$; and for the positive-energy intermediate state only, $N=1$.

[12] M.-T. Noda (private communication).

We have found empirically an efficient alternative to matrix inversion for solution of these equations. By iteration of the equations to obtain the coefficients of $(g^2/4\pi)^n$ in the power series for $\tan\delta$, the Padé approximant to $\tan\delta$ can be formed. It is found that for the same mesh the Padé method reproduces the solution by matrix inversion to any desired accuracy by choice of a sufficiently high approximant. Thus by using the Padé method, the coefficients need only be found once to obtain the solution, although the order of the approximant required depends upon $g^2/4\pi$. This contrasts with the matrix-inversion method which must be repeated for each value of $g^2/4\pi$.

No effort has been made to extend this calculation beyond the pion-production threshold. At the threshold the interaction develops a singularity and the equations can no longer be easily broken down into purely real and imaginary parts.

This method can be extended to the $J\neq0$ cases, but it becomes more complicated due to the increase in the number of intermediate states. For the $J=1$ case, one must deal with the $^3S_1$, $^3D_1$, $^3P_1$, and $^1P_1$ states, and upon an analysis similar to that in Sec. II, it is found that eight intermediate states are possible. However, once the $J=1$ problems are conquered, all other cases are completely analogous.

The original goal of this program was the production of the amplitudes of the ladder graphs and this has been achieved with an accuracy of about 20% up through the five-pion-exchange graph.

ACKNOWLEDGMENT

The authors are indebted to Professor John Nuttall for several valuable discussions.